ROLE OF MODEL IDENTIFICATION AND ANALYSIS METHOD IN THE SEISMIC ASSESSMENT OF HISTORICAL MASONRY TOWERS

Maria Cristina Porcu[1*], Elisa Montis[1], Manuel Saba[2]

[1]Dept. of Civil Engineering, Environmental Engineering and Architecture, University of Cagliari, via Marengo 2, 09123 Cagliari, Italy.

[2]Research Group ESCONPAT, Faculty of Engineering Universidad de Cartagena, Cra. 6 #36-100, Cartagena, Colombia.

*Corresponding Author: mcporcu@unica.it

Abstract

The seismic assessment of historical monuments typically involves many issues, the most crucial of which are: retrieving geometrical and mechanical data; implementing a suitable numerical model; choosing the more appropriate type of analysis and properly interpreting the results. The more well-managed these issues are the better the reliability of the seismic assessment. The Civic Tower of L'Aquila (Italy) is considered in this paper as a typical case in which lack of data and discrepancy of sources make the seismic assessment hard to be suitably performed. The key role of the identification of the numerical model was firstly evidenced. Different numerical models were implemented to identify the best-fitting geometrical and mechanical properties of the structure. The considered case-study also led to the discussion of some issues concerning the identification of the numerical model of historical towers. Code-compliant linear and non-linear dynamic analyses were then carried out to compare the seismic performance of the tower assessed through the different methods based on regulations. A concrete damage plasticity model for masonry and a set of spectrum-consistent earthquakes were adopted. The stress maps, the horizontal displacement peaks (useful to avoid the pounding phenomenon with the adjacent Margherita palace), and the evolution of damage were investigated. The study highlighted that the widely adopted response-spectrum modal analysis (RSMA) may underestimate -even remarkably- the displacement demand compared to the more rigorous time-history linear analysis (THLA), this being an inconsistency of the code-compliant linear analyses. On the other hand, the results of the non-linear time-history analysis (NLTHA) confirmed the displacement demand predicted by the THLA, while the damage evolution under tensile stress was found in agreement with the crack pattern detected on the structure. The influence of the vertical component of the earthquake was also investigated, founding that the vertical component of the ground motion does not significantly affect the results.

Keywords: seismic assessment, historical masonry towers, dynamic time-history analyses.

1. Introduction

The seismic assessment of historical buildings is of key importance in earthquake-prone countries where the presence of ancient monuments is widespread [1][2][3]. Although a good seismic performance and even a ductile behaviour is sometimes exhibited by ancient structures built according to empirical rules [4], historical buildings are usually hardly able to withstand strong horizontal forces. To study the seismic performance of a historical structure a suitable numerical model is needed, which calls for a preliminary knowledge of the system's full geometry and mechanical properties. Achieving a good level of such preliminary knowledge is not an easy task, due to difficulties in the complete accessing of the structure and/or in carrying out in-situ experimental tests. The identification process, based on comparing experimental and numerical modal parameters, may significantly help to obtain a reliable numerical model of an existing structure when lack of data and incoherence between sources occur [5]. Such a process typically entails approximations and assumptions that should be appropriately made.

The Civic Tower of L'Aquila has been considered here as a noteworthy case-study. Despite the many available experimental and numerical investigations [6][7][8][9][10][11][12], some uncertainties still remain about the geometrical and mechanical properties of this Medieval Italian monument. Based on the literature sources and on supplementary data provided by the Municipality of L'Aquila, different detailed and representative three-dimensional finite-element models of the tower are developed in this study, in order to identify the best fitting geometrical and mechanical properties of the system. The considered case-study gives insights to show how the modal identification procedure may be able to dispel doubts about structural features otherwise unknowable. On the other hand, it also highlights some criticisms that may affect the identification process when ancient masonry towers are concerned. This matter is addressed in the paper.

By referring to the identified model of the case-study tower, the paper then investigates the impact of the analysis method on the efficacy of the seismic assessment of ancient monuments. Different analysis techniques are in fact allowed by design regulations [13][14] to assess the seismic behaviour of new or existing structures, some of them being more approximate and easier to apply, some others more rigorous but time-consuming. One of the most used in practice is the Response Spectrum Modal Analysis (RSMA), which is an approximate linear dynamic approach often elected as the reference method by the regulations. A more accurate approach is the Time-History Linear Analysis (THLA), based on the numerical integration of linear differential equations under spectrum-consistent ground motions. Non-linear analyses are more adept, however, to study the seismic response of masonry structures, able as they are to account for

asymmetric constitutive behaviour in tension and compression. A Time-History Non-Linear Analysis (THNLA) under spectrum-consistent earthquakes is, in fact, the most accurate way to explore the post-elastic, dissipative and ductile behaviour of structures [15][16][17][21]. A high computational burden and considerable expertise are, however, needed to achieve such an accuracy [19]. It should also be mentioned that an incremental dynamic analysis, performed under earthquakes of different scaled intensity, can be also used to study the global collapse capacity of structures [20].

Many studies investigated the seismic performance of historical Italian masonry towers, cf. e.g. [21-31]. Some of them referred to simplified methods or pushover analyses to assess the seismic vulnerability of existing structures [21-22] or to investigate the reliability of different numerical models with increased details [23]. Some others carried out full dynamic non-linear analyses under artificial design-consistent or real earthquakes to assess the role of geometry on the seismic behaviour of masonry towers [24]; to investigate the effectiveness of advanced numerical simulations of the masonry behaviour [25]; to assess the role of different parameters on the seismic vulnerability of 3D simplified models of masonry towers [26] or to study the evolution of damage in structures hit by recent events [29]. A comparison between the results of non-linear static (pushover) and full non-linear dynamic analyses was made in [27-28]. Linear and non-linear methods of analyses were adopted in [30] to assess the efficacy of different rehabilitation strategies. The present study aims to provide a further contribution to the field by comparing the effectiveness of the results obtained from the different kinds of dynamic analyses (RSMA, LTHA and NLTHA) allowed by the Italian regulation and the European code.

An RSMA is firstly performed to study the seismic behaviour of the L'Aquila tower for the collapse-prevention and life-protection ultimate limit states, according to EC8 [14] and to the Italian Building Code [13]. Linear time-history analyses are then carried out with two sets of seven earthquakes consistent to the design spectra relevant to the life protection and the collapse prevention limit states respectively. The displacement demand is estimated under all the considered earthquakes for each limit state and compared with that obtained from the RSMA. Non-linear time-history analyses under the strongest earthquake of the two sets are also carried out to assess displacement demand and damage propagation under extreme conditions. A rough estimate of the joint depth to prevent pounding effects between the tower and the adjacent Margherita palace is also provided in the study. The pounding between adjacent structures assumes in fact a key role in the seismic assessment of historical buildings. The problem is of paramount importance when structures of different height are involved since they may oscillate with rather different fundamental frequencies, as typically happens when a tower and adjacent lower buildings are concerned [32][32].

Depending on the level of accuracy required, different approaches can be followed to model masonry for a numerical analysis [32][33], the more simplified the modelling approach the less demanding the analysis. Macro-modelling is the most suitable approach to study the performance of large structures. It was adopted in the present study, which considers masonry as a continuum medium, characterized by homogenous and averaged properties, as often done in the literature [21][21] [25][27]. Discontinuous approaches in which the seismic behaviour of Medieval masonry towers is studied through a 2D or 3D detailed discretization based on rigid blocks and deformable joints have been also developed [24] [25]. The Concrete Damage Plasticity (CDP) model is introduced in the present investigation to represent the non-linear constitutive stress-strain relationship of the masonry, this model being often adopted when modelling ancient towers [21] [30].

The effect of the vertical component of the earthquakes is also evaluated both in the linear and non-linear analyses. Some studies evidenced, in fact, that this component can affect the seismic response of slender tall structures [25] and modify the damage propagation in masonry ancient towers [34]. The present study investigates whether the vertical ground motion can significantly affect stress, displacements and damage propagation when this kind of structures are concerned.

2. Identification procedure

2.1 Case study: Civic Tower of L'Aquila

The Civic Tower of L'Aquila is a tall and slender masonry structure, built in the thirteen century (between 1254 and 1374) with an original height of 70 m, that was lowered during historical reworking to about 40 m, see Fig.1a, [6][7][8]. A surviving bell of two originals is located at the top of the tower. Limestone squared blocks (about 0.70 m wide, 0.45 m high) characterize the outer tower's façade [7], while, presumably, a sack masonry characterizes the internal structure of the walls, as typical in these kinds of historical monuments.

The town of L'Aquila belongs to a high-seismicity Italian area, see Fig.1b, and, in fact, such a medieval monument suffered many seismic events during its life, the most violent of them having occurred in 1703 and in 2009, respectively. The tower has undergone structural changes and restorations during its life; to strengthen the structure, steel tie rods have been recently inserted to connect the orthogonal walls (visible in Fig.1a). Adjacent to the tower is *Margherita palace*, see Figs 1a and 1c, a 15.22 m high masonry building that was built in the XIII century [6] [7]. The palace and the tower border along two sides (cf. Fig.1d), in the west-east and north-south directions (taken in the following analysis as x and y directions, respectively).

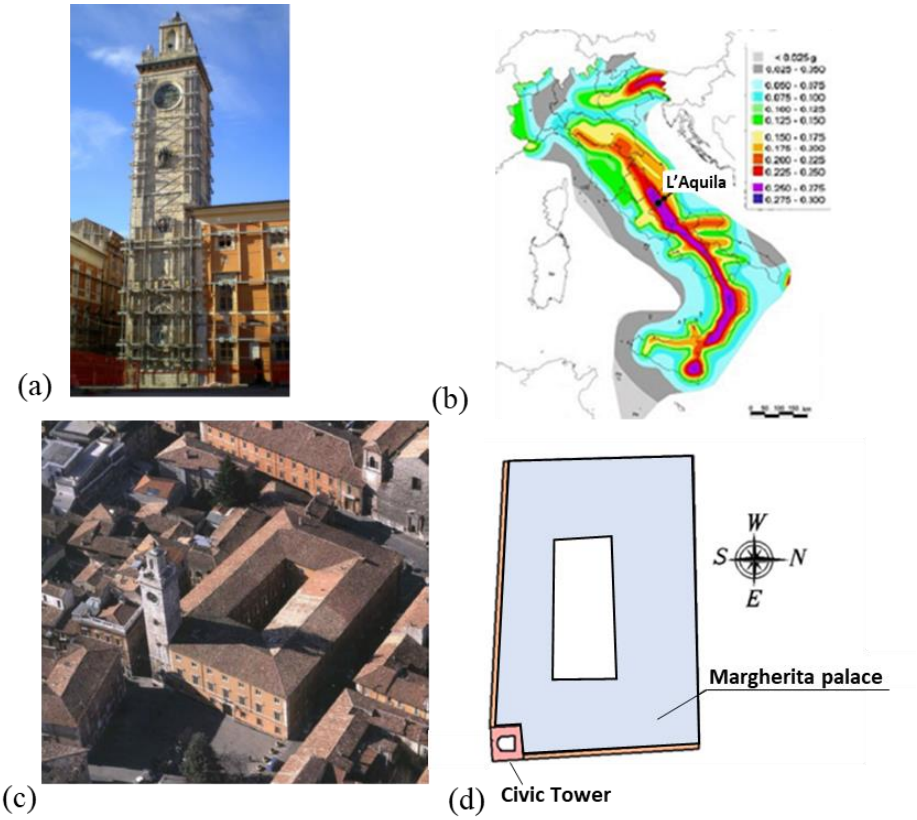

Figure 1. (a) Civic Tower of L'Aquila with post-earthquake temporary metallic bracing and the adjacent Margherita palace; (b) Italian seismicity map; (c) view from above; (d) schematic plan.

2.2 Geometrical models

A wide preliminary study of the historical and bibliographical sources [6][7][8][9][10][11] was performed to investigate the tower's geometry and materials. Lack of data and discrepancies between sources were found. Base dimensions of the walls and tapering of them upwards are some of the aspects ambiguously stated. Scarce data about the materials are also available. On the other hand, an internal inspection of the monument and tests on the structure are not currently possible. Thanks to recent dynamic tests [9], [10] carried out on the structure, an identification process of the numerical model was exploited to decide the best representative geometry and the best fitting mechanical properties of the masonry.

Based on the available data, three different detailed geometries of the tower were considered. They are displayed in Fig. 2 and referred to as M1, M2 and M3. The geometry of M1 is taken from [7], where some data are obtained through laser-scanner tests at the base of the tower. The second geometrical scheme of the tower, M2, was considered according to [8][9] instead. A slightly different base section belongs to geometrical models M1 and M2, say *Base section B1* for M1 and *Base section B2* for M2, the two models also differing for the vertical section of the walls, constant in M1 and tapered upwards in M2, see Fig.2. Single-leaf walls were assumed in

the numerical model as an approximation, due to the fact that the actual internal structure of the masonry walls is unknown.

As a matter of fact, the hypothesis of the thickness of walls that narrows upwards (tapered walls) made in [8][9] seems to be more realistic than that of a constant wall thickness assumed in [7]. Tapered walls are in fact typical of similar Italian medieval towers [5][27]. On the other hand, base section B1 appears to be the most accurately measured [7]. Therefore, a third model was finally considered in the present paper, referred to as M3 in Fig.2. The same base section of M1 belongs to M3, which, in contrast to M1, is made of walls tapered upwards as M2. The identification process showed eventually that model M3 is the best-fitting one.

Two clay/cement mix slabs and a wooden slab (made by wooden trusses, planking and tiles) are present in the three geometrical models, as indicated in Fig. 2.

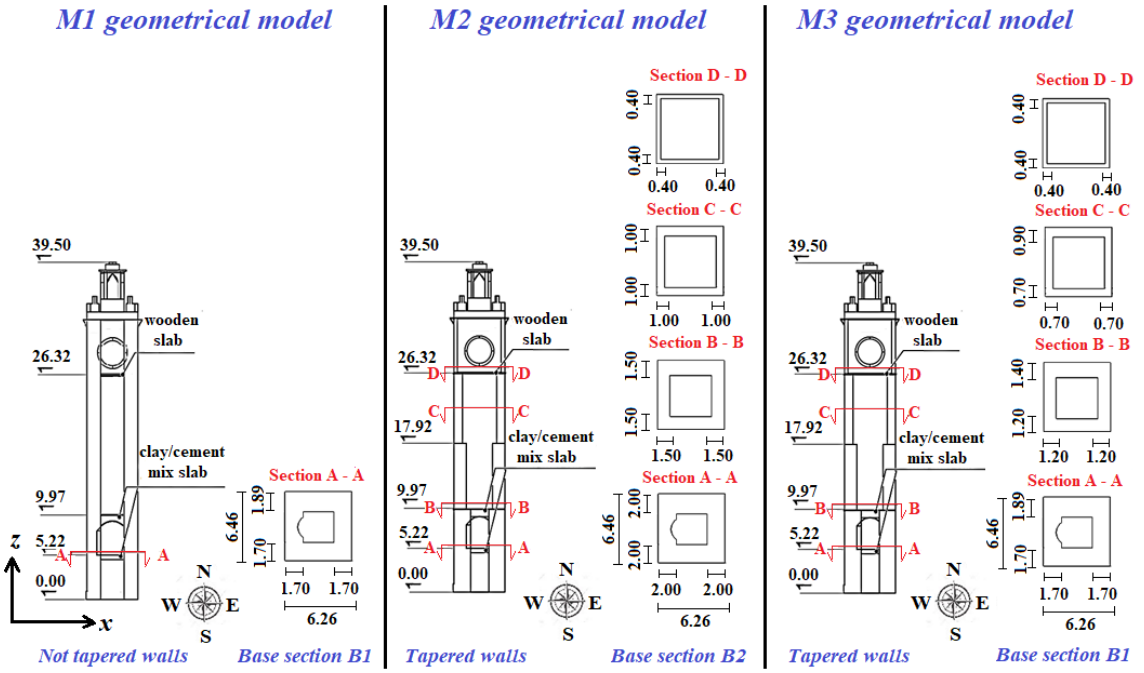

Figure 2. *Three geometrical schemes of the tower, the first two derived from literature sources and the third one proposed in the present paper (dimensions in meters).*

2.3 Numerical models

Based on the schemes given in Fig. 2, detailed geometrical models were built in a computer-aided design environment (CAD) and then numerical models have been implemented in the commercial software ABAQUS [34], see Fig. 3. Tetrahedral 3D ten-nodes elements (C3D10) were adopted to model both the masonry and the slabs. The hypothesis of a perfect embedment at the base of the tower was made [7], while the interaction with the adjacent Margherita Palace was neglected. Homogeneous isotropic continuous materials with linear indefinitely elastic behaviour were

initially assumed to carry out modal and linear seismic analyses. A more realistic non-linear behaviour of the masonry was successively considered to perform the THNLA, as described in Section 4. An increasing discretization (mesh) refinement was performed for all the considered models.

2.4 Identification of the best-fitting numerical model

Since no definite data about the mechanical and inertial properties of the masonry walls were available, an identification procedure was performed by referring to conventional ranges of values for the compression strength f_m, the Young's modulus E, the shear modulus G and the mass density γ in agreement with the Italian code [13], see Table 1. The conventional values of elastic moduli and mass density given in Table 2 were assumed for the slabs. The thickness t of each slab is also provided in Table 2, as obtained by in situ measurements [7].

Table 1. Conventional mechanical properties of squared stone block masonry [13]

f_m [MPa]	E [MPa]	G [MPa]	γ [kN/m^3]
6-8	2400÷3300	780÷940	19÷22

Table 2. Properties of the slabs

Slab type	t [m]	E [N/mm^2]	G [N/mm^2]	γ [kN/m^3]
Clay/cement mix Slab (1° story)	0.5	7355	2828.8	18.00
Clay/cement mix Slab (2° story)	0.9	7355	2828.8	18.00
Wooden Slab	0.12	10100	3884.6	8.25

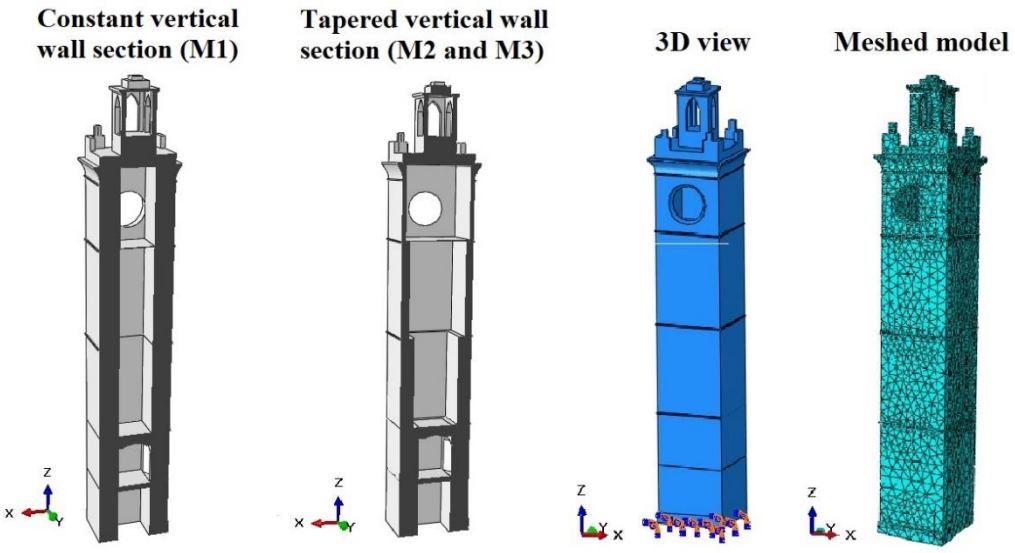

Figure 3. *Vertical sections and 3D views of the FEM models implemented.*

To find the most realistic geometry of the tower among those displayed in Fig. 2, and the best-fitting properties of the masonry in the ranges of values given in Table 1, tentative values of E and γ were considered for each of the geometrical models in Fig. 2, while the value of G was directly obtained though the well-known relationship $G = E/(2(1+\nu))$; the value of the Poisson ν ratio being taken as $\nu = 0.3$. A damping ratio $\xi = 5\%$ was assumed for all modes, which is a realistic value for masonry, and the Rayleigh proportional damping coefficients were calculated accordingly.

The identification process was carried out by comparing the first natural frequencies of the numerical models with the experimental ones, the latter being taken from the results of two different experimental campaigns carried out by Cimellaro et al. in 2009 (after the April earthquake) [9] and by Lorenzoni et al. in 2010 [10]. The first five experimental frequencies, detected in [9] and in [10] under ambient vibration tests, are listed in the second and third row of Table 3 respectively. The frequencies found in the two studies are in agreement with each other, although slightly higher values are detected by Lorenzoni. Moreover, a little difference between the frequencies in the two orthogonal directions (N-S, E-W) for the bending first-mode and for the bending second-mode was found by Lorenzoni et al. This difference is in fact compatible with the different size of the horizontal section in the two directions, namely 6.26 m in x-direction and 6.46 m in y-direction, see Fig. 2.

A step-by-step iterative procedure was performed to minimize the discrepancy between the experimental first frequencies and the numerical ones. The procedure was carried out for the three different geometries and by varying the values of the elastic modulus E and of the mass density γ within the ranges given in Table 1. At the end of this investigation it was found that model M1, characterized by non-tapered walls (Fig.2), was not representative of the dynamic behaviour of the tower. In fact, far too low values of frequency belong to this model, the first frequency ranging between 1 Hz to 1.2 Hz for elastic modulus values assumed in the range of Table 1. This led to exclude that the tower's walls have a constant section along the height, as was assumed in [7].
Both tapered upwards, models M2 and M3 (see Fig. 2), better matched the flexional frequencies found with the experimental modal analysis. Model M3 was, however, finally assumed to be the best representative model of the tower, provided that the updated material properties given in Table 3 were adopted. The first five meaningful frequencies of this model are listed in the last column of Table 4, while the shapes of the first five modes are displayed in Fig.4.

Table 3. Identified masonry properties for the M3 model

E [MPa]	G [MPa]	γ [kN/m^3]
3286.50	1264	19

Table 4. Experimental and numerical first five frequencies of the tower

Mode	Experimental frequencies (Hz)		Numerical frequencies (Hz)
	Cimellaro [9]	Lorenzoni [10]	Identified M3 model
1st bending N-S	1.48	1.56	1.48
1st bending E-W	1.48	1.58	1.53
2nd bending N-S	3.24	3.30	5.80
2nd bending E-W	3.20	3.71	6.03
1st torsional	4.22	4.51	6.17

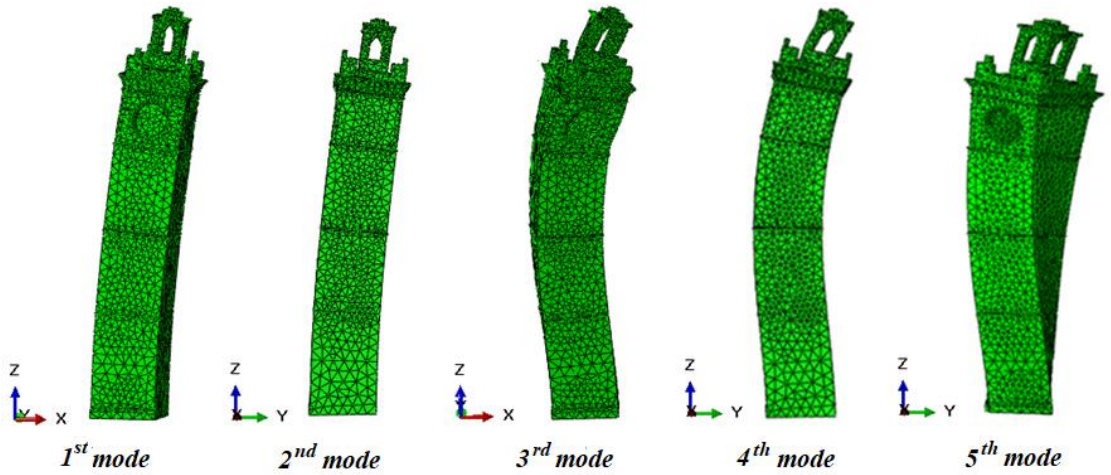

Figure 4. *First five mode shapes of the tower.*

2.5 Some insights about the modal identification of masonry towers

The comparison presented in Table 4 shows a good agreement between the first two numerical and experimental frequencies in the main directions. The corresponding fundamental periods (0.65 s and 0.67 s) are in the range of the expected values for this kind of structures, depending on their height [36]. As far as the 2nd bending modes and the 1st torsional mode are concerned, however, a discrepancy between numerical and experimental frequencies was found (see Table 4). Indeed, the model appears to be stiffer than the actual structure for such modes. This discrepancy might be due to several factors and overcome in different ways. Some insights are drawn below.

i. Among the possible causes of the lack of identification of higher modes, the heterogeneity of the materials along the tower's height and the lack of integrity of parts of the walls (due to widespread presence of cracks) [8] can be cited. The latter,

in particular, introduces non-linearity and increases the anisotropy effects, lowering the values of the higher frequencies compared to those of the linear isotropic model, as discussed in [23]. It was also shown in [23] that it is not possible to obtain a proper value of the torsional mode frequency (the fifth in Table 4) of an ancient masonry tower if pre-existing cracking and anisotropy of the masonry are not considered explicitly in the numerical model [23].

ii. Accounting for anisotropy and inhomogeneity of the material along the height could lead to a better identification of the frequencies higher than the first two. An approach to do this can be that of subdividing the tower into distinct portions along the height and assigning different elastic moduli to the walls of the different portions, the moduli values being calibrated through an iterative identification procedure also involving the higher frequencies. Such an approach was recently proposed in [27] where it led to an excellent identification of the first four frequencies of ancient masonry towers. Other approaches were devoted instead to introducing the presence of cracks in the masonry. For instance, in [23] this was done by means of a simplified elastic approach where the horizontal Young modulus was reduced by a damage parameter the value of which should be identified. This approach was based on the assumption that cracks are typically subvertical and thus the vertical modulus was kept unchanged. The downside of these otherwise powerful procedures is that they are very cumbersome and time-consuming.

iii. It can be also argued that the L'Aquila tower is not an isolated structure as assumed in the present study for the sake of simplicity, but it is partially bounded by the Margherita palace (Fig.1d). This could be a further cause of non-full modal identification. The tower and the palace were built at different times and very presumably their walls are structurally separated. Nevertheless, the presence of the palace provides a sort of constraint along two sides of the tower. Estimating the restraint degree offered by the palace and duly introducing it in the tower's model is surely a highly demanding task. To face it, portions of the building adjacent to the tower might be added to the model, the elastic modulus of such portions being reduced by a factor to be identified, as done in [36]. Accordingly, an attempt to account for the presence of the palace was made in this study by adding some horizontal springs at the level of the palace roof, the stiffness constants being taken as parameters to be determined through the identification procedure. However, this approach was unsuccessful since the values of higher frequencies did not drop enough while keeping the fundamental frequencies in the two main directions still identified. As a matter of

fact, the modal identification approaches are typically performed in the elastic field, and this is a limit when inherently inelastic materials like damaged historical masonry are concerned, as stressed in [36].

iv. A full tower+palace model would be even implemented to account for the dynamic interaction between the two structures. This would considerably increase the effort of modelling, identification and analysis, while again entailing uncertainties about the constraints to insert between the two structures. On the other hand, a more detailed model is not always the best way to achieve the set goals.

v. It is well known that the contribution of higher modes becomes more and more neglectable when linear approaches are concerned. On the other hand, when a non-linear behaviour is considered, the more the system enters the plastic range the less the response is affected by the dynamic effects occurring in the elastic range [38]. This could justify giving minor relevance to the identification of higher modes.

vi. Considering the structure stiffer than the actual one for the higher modes would lead to more conservative results, at least when linear analyses are concerned. In fact, higher values of frequencies mean lower values of period which in turn typically imply higher spectral accelerations (peak zone of the design spectrum) and thus higher seismic actions.

It should be stressed finally that the full identification of the L'Aquila tower is beyond the purposes of this study, the main aims of which are presenting some insights about the role of the identification process for ancient masonry towers and investigating the effectiveness of the different dynamic methods of analysis allowed by regulations to assess the seismic behaviour of these structures. Therefore, M3 model is finally adopted in the study. Since the same model was used when applying all the considered analysis methods, the findings of the presented comparison can be considered valid and not affected by the non-full identification of the model with respect to the real monument.

3. Response spectra and spectrum-consistent earthquakes

Relevant to L'Aquila, the design response spectra for the ultimate limit states of Life Protection (LP) and Collapse Prevention (CP) requirements were built according to the Italian code [13] and Eurocode 8 (EC8) [14]. They are displayed in Fig.5a and Fig.5b for the horizontal and the vertical components. Two spectra are provided for the LP limit state, the lower one (blue curve) being obtained from the higher one (light blue curve) through the reduction factor q. The reduced LP

spectrum is used to carry out the RSMA, while the unreduced LP spectrum is taken as target to find consistent earthquakes for the time-history analyses.

It should be noted that, according to the Italian [13] and European [14] code rules, the effects of the earthquake's vertical component would not need to be taken into account for structures like the one under consideration. However, some studies, [25] [34], recently highlighted the role of the vertical component of the earthquake on the seismic behaviour of slender tall structures. Thus, the effect of the vertical component on the seismic response of L'Aquila tower was also investigated in this study.

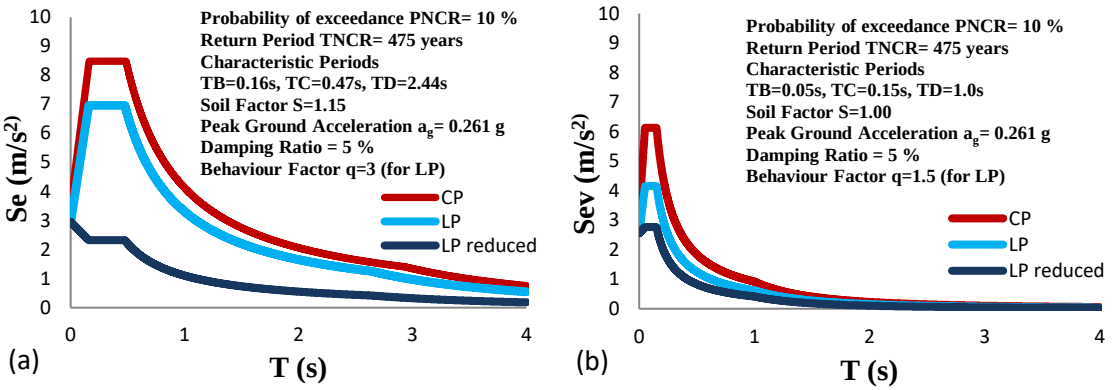

Figure 5. *(a) Horizontal design response spectra; (b) vertical design response spectra.*

Italian regulation [13] and EC8 [14] provide a guide to select spectrum-compatible ground motions, ensuring that the maximum effects produced by the accelerograms are in line with the maximum effects produced by the target spectrum. Two sets of seven spectrum-consistent earthquakes were extracted by means of the software REXEL [38], the former for the LP limit state and the latter for the CP limit state respectively. Reference to the European Strong Motion Database [40] was made while a magnitude range $6 \leq M_w \leq 7$ and an epicentre distance $\Delta \leq 30\ Km$ were assumed. For the two horizontal components, the upper and lower tolerated deviation of the average spectrum from the target spectrum were set to 10 % and 30 % respectively. Both the Italian Building Code [13] and EC8 [14] set 10% as maximum lower tolerance, while no indication about the upper deviation is provided by EC8, which can lead to inconsistencies in the analysis [41][4]. A 30 % limit to the upper tolerance was recently introduced by the Italian code [13] instead. To consider very strong vertical actions, an upper tolerated deviation of 50 % was set in the present study for the vertical components of both the two sets of earthquakes.

The target spectrum, the spectra of the seven couples of selected horizontal records, their averaged spectrum, and the lower and upper tolerance are plotted together in Figures 6a and 6b, as obtained from Rexel for the LP and CP limit states respectively. Figures 7a and 7b provide

similar diagrams relevant to the vertical components. Table 5 summarize the two sets of seven earthquakes used in the time-history analyses. It should be noted that three earthquakes (namely EQ3, EQ5 and EQ7) appear in both the sets. In total eleven different earthquakes are considered in the analyses. All the records considered in the three directions are plotted in Figures 8-10.

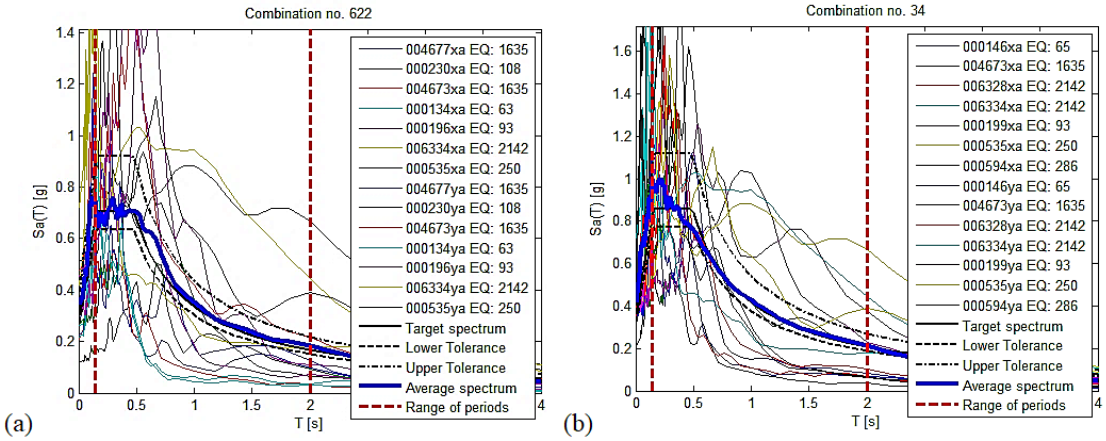

Figure 6. *Spectra of the couples of horizontal records, average spectrum, target spectrum with upper and lower tolerance, relevant to the (a) LP limit state and (b) CP limit state.*

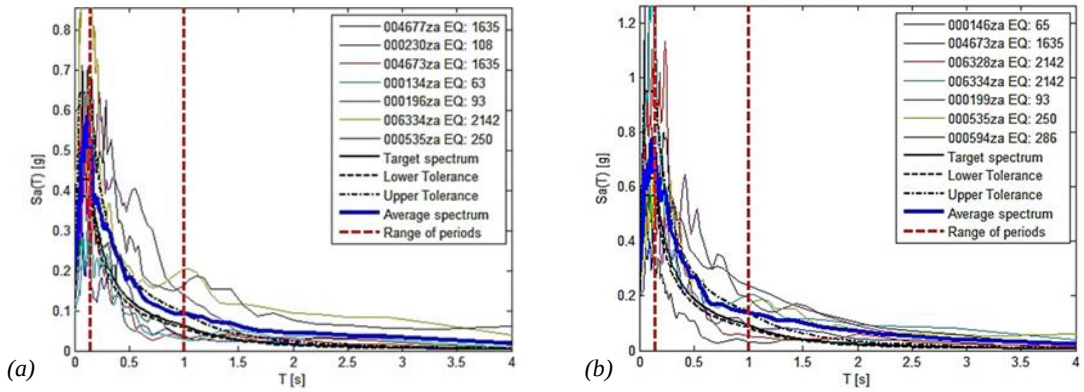

Figure 7. *Spectra and average spectrum of the vertical records, target spectrum with upper and lower tolerance, relevant to the (a) LP limit state and (b) CP limit state.*

Table 5. Horizontal and vertical records considered in the two ultimate limit state analyses

Ultimate limit state	Earthquake	X component	Y component	Z component
Life protection (LP)	***EQ 1***	134 xa EQ 63	134 ya EQ 63	134 za EQ 63
	EQ 2	196 xa EQ 93	196 ya EQ 93	196 za EQ 93
	EQ 3	535 xa EQ 250	535 ya EQ 250	535 za EQ 250
	EQ 4	230 xa EQ 108	230 ya EQ 108	230 za EQ 108
	EQ 5	4673 xa EQ 1635	4673 ya EQ 1635	4673 za EQ 1635
	EQ 6	4677 xa EQ 1635	4677 ya EQ 1635	4677 za EQ 1635
	EQ 7	6334 xa EQ 2142	6334 ya EQ 2142	6334 za EQ 2142
Collapse prevention (CP)	***EQ 8***	146 xa EQ 65	146 ya EQ 65	146 za EQ 65
	EQ 9	199 xa EQ 93	199 ya EQ 93	199 za EQ 93
	EQ3	535 xa EQ 250	535 ya EQ 250	535 za EQ 250
	EQ10	594 xa EQ 286	594 ya EQ 286	594 za EQ 286
	EQ5	4673 xa EQ 1635	4673 ya EQ 1635	4673 za EQ 1635
	EQ 11	6328 xa EQ 2142	6328 ya EQ 2142	6328 za EQ 2142

	EQ7	6334 xa EQ 2142	6334 ya EQ 2142	6334 za EQ 2142

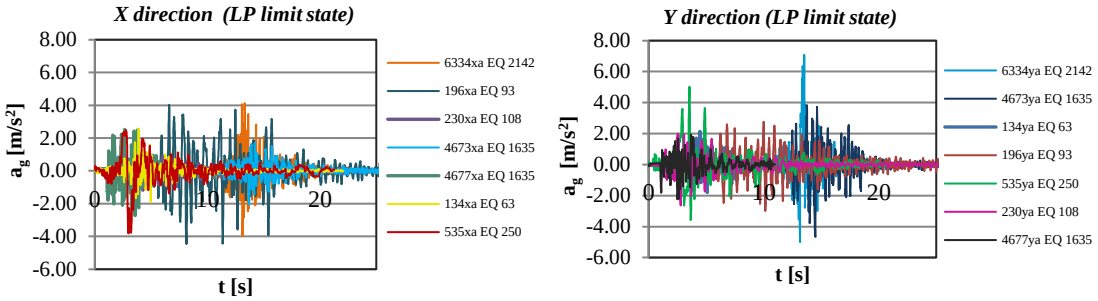

Figure 8. *Set of horizontal spectrum-consistent records for the LP limit state. (a) X direction, (b) Y direction*

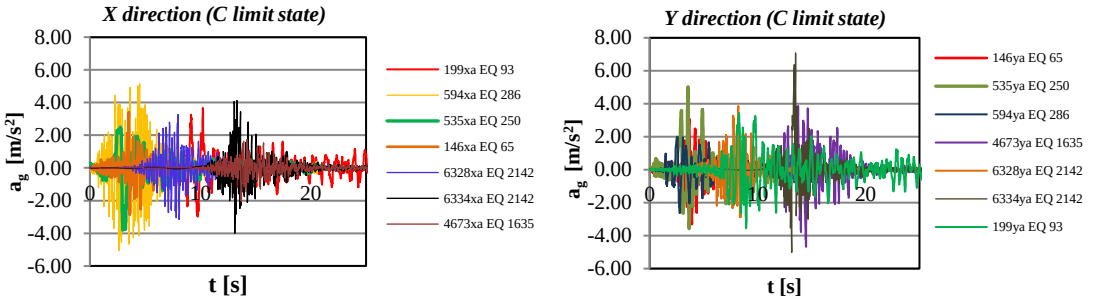

Figure 9. *Set of horizontal spectrum-consistent records for the CP limit state. (a) X direction, (b) Y direction*

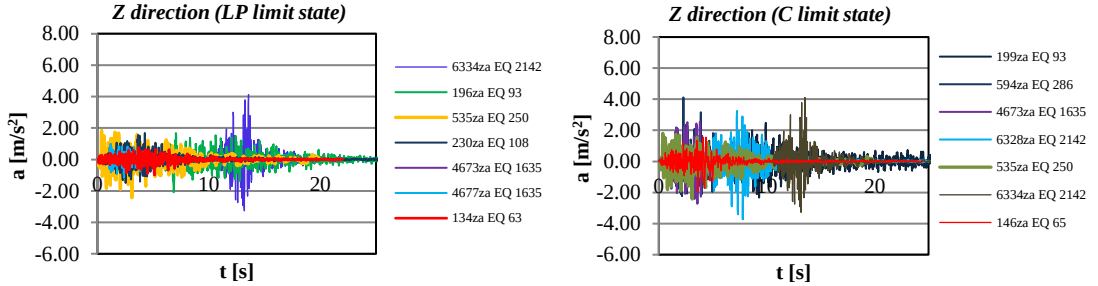

Figure 10. *Set of vertical spectrum-consistent records for the (a) LP limit state and (b) CP limit state.*

4. Linear analyses

Performing a linear analysis implies assuming a reversible linear elastic behavior of the materials both to compression and tension but this is hardly realistic for most materials. Masonry has an asymmetric non-linear behavior being almost unable to resist tensile loads. To take this asymmetric non-linear constitutive behavior into account, a suitable stress-strain curve should be introduced in the numerical model, and a non-linear analysis should be carried out as done in

Section 5. Linear analyses can, however, get an idea of the seismic performance of the tower provided that the results be carefully checked and interpreted.

Two kinds of code-compliant linear dynamic analyses were carried out in the present study: the Response Spectrum Modal Analysis (RSMA) and the Time-History Linear Analysis (THLA), both applied according to the Italian code [13] and to EC8 [14]. To check the impact of the vertical component of the earthquake on the results, RSMA and THLA were carried out twice, once neglecting and once considering the vertical component of the earthquake.

4.1 Response Spectrum Modal Analysis (RSMA)

An RSMA was carried out with reference to the design spectra given in Fig. 5. According to EC8 [14], all modes with a participant mass greater than 5% and as much modes as needed to sum up 90% of the total mass were considered (it is to note that 85 % of the total mass would be enough for the Italian code, [13], while EC8 recommends to reach at least 90%). The first 16 modes were considered, which summed up about 95% in the x direction, 95% in the y direction and 94% in the z direction, respectively.

The maximum displacements at the top of the tower (namely at a height of 39.50 m) and at the level of the roof of Palazzo Margherita (15.22 m) in the x and y direction, are listed in Table 6 for the two ultimate limit states. The vertical component of the earthquake was found to not affect the values of the horizontal displacements of the tower. It is worth noting that the tower's displacements at the level of the roof of Palazzo Margherita are useful to assess the pounding phenomenon between the tower and the palace.

Table 6. *Maximum displacements of the tower obtained from MRSA.*

Limit state	**Tower level**			
	15.22 m		39.50 m	
	Ux (m)	Uy (m)	Ux (m)	Uy (m)
LP	0.020	0.020	0.083	0.080
C	0.026	0.025	0.104	0.100

The displacement values relevant to the LP limit state given in Table 6 are calculated by means of the following procedure. Since the LP design spectrum adopted for the RSMA is obtained by scaling the elastic spectrum through the behaviour factor q (see Fig. 5), the total horizontal displacement d_E relevant to the LP limit state must be obtained by multiplying the displacement d_{Ee} derived with reference to the reduced spectrum, by a corrective factor μ_d, according to codes [13] [14]:

$$d_E = \pm \mu_d d_{Ee} \tag{1}$$

where:

$$\begin{cases} \mu_d = q & if\ T_1 \geq T_C \\ \mu_d = 1 + (q-1)\, T_C/T_1 & if\ T_1 < T_C \end{cases} \quad (2)$$

Here T_1 is the fundamental period of the structure while T_C is the period at which the constant horizontal part of the design spectrum halts. Being in this case $T_1 \geq T_C$, formula $(2)_1$ is applied to obtain the displacement values given in Table 3 for LP.

It should be stressed that the seismic stresses obtained through the RSMA are not combined to those due to the dead loads by ABAQUS, this being a sort of deficiency of the software. For this reason, neither the stress resulting from the RSMA (with and without the vertical component of the earthquake) nor their comparison with the stresses obtained from the THLA are here presented. On the other hand, investigating on the stress demand is not useful when a reduced design spectrum is adopted. The displacement demand is more significant, in fact, and the horizontal displacements are not affected by the above-mentioned lack of the software.

4.2 Time-History Linear Analysis (THLA)

A THLA was carried out under each of the earthquakes listed in Table 5. The analyses were performed both with and without the vertical component of the earthquake. Since three of the 14 earthquakes are common to the two sets, 22 THLAs were carried out overall with 11 different earthquakes (see Table 5). The results obtained for each limit state were averaged over the seven earthquakes of the set, as suggested by EC8 [14]. Table 7 provides the maximum vertical stresses (compression and tension) obtained from the different analyses. The stress increment due to the vertical component of the earthquake is provided in the last two columns of the same table. It can be noted that, on average, the stress increment is less than 5% for the LP limit state and less than 7% for the CP limit state.

Table 7 shows that the stress demand is very high, even on average. The values reached in compression exceeded the yield value (6 MPa) assumed in Section 5 for the masonry and are very close (even exceeding it in the CP limit state) to the stress peak assumed for the hardening branch (8 MPa) of the stress-strain constitutive diagram in Figure 16a. The highest concern is however about tension stresses which are markedly higher than the tensile yield limit assumed for the material (0.6 MPa in Figure 16b), masonry being in fact typically very poorly resistant to tension. This of course predicts the presence of widespread cracks in the real structure after earthquakes consistent with both the LP and CP design spectra.

Table 7. *Maximum vertical stresses obtained from the THLAs*

Limit state	Earthquake for THLA	Vertical component of the earthquake		Stress increment
		NO	YES	

		Tension (MPa)	Compression (MPa)	Tension (MPa)	Compression (MPa)	Tension (%)	Compression (%)
LP	EQ 1	0.3	1.72	0.31	1.73	3.33	0.58
	EQ 2	11.26	12.11	11.34	12.56	0.71	3.72
	EQ 3	8.58	9.06	9.42	9.69	9.79	6.95
	EQ 4	4.91	7.33	4.96	7.41	1.02	1.09
	EQ 5	4.35	6.11	4.37	6.12	0.46	0.16
	EQ 6	1.19	5.45	1.26	5.94	5.88	8.99
	EQ 7	6.45	9.09	7.22	9.55	11.94	5.06
	Average	**5.29**	**7.27**	**5.55**	**7.57**	**4.73**	**3.79**
CP	EQ8	3.05	5.45	3.09	5.51	1.31	1.10
	EQ9	9.10	11.22	9.92	11.75	9.01	4.72
	EQ3	8.58	9.06	9.42	9.69	9.79	6.95
	EQ10	7.34	7.95	7.45	8.06	1.50	1.38
	EQ5	4.35	6.11	4.37	6.12	0.46	0.16
	EQ11	2.59	5.45	2.83	5.51	9.27	1.10
	EQ7	6.45	9.09	7.22	9.55	11.94	5.06
	Average	**5.92**	**7.76**	**6.33**	**8.03**	**6.85**	**3.42**

Table 8 provides the maximum displacements obtained from the different analyses and the averaged values for each set. As for the RSMA the horizontal displacements were found to be not affected by the vertical component of the earthquake. It can be noted that on average a very similar displacement demand was found for the CP and LP limit state. The comparison between these results and those obtained from the RSMA will be discussed in Section 4.3.

Table 8. *Maximum displacements of the tower obtained from the THLAs*

Limit state	Earthquake for THLA	Tower level			
		15.22 m		39.50 m	
		Ux (m)	Uy (m)	Ux (m)	Uy (m)
LP	EQ 1	0.014	0.020	0.018	0.033
	EQ 2	0.084	0.036	0.249	0.120
	EQ 3	0.306	0.184	0.398	0.297
	EQ 4	0.04	0.063	0.090	0.138
	EQ 5	0.028	0.100	0.040	0.139
	EQ 6	0.041	0.049	0.053	0.074
	EQ 7	0.135	0.248	0.153	0.350
	Average	**0.093**	**0.100**	**0.143**	**0.166**
CP	EQ8	0.029	0.033	0.054	0.076
	EQ9	0.106	0.154	0.193	0.227
	EQ3	0.306	0.184	0.398	0.297
	EQ10	0.05	0.047	0.120	0.112
	EQ5	0.028	0.100	0.040	0.139
	EQ11	0.046	0.051	0.061	0.083
	EQ7	0.135	0.248	0.153	0.358
	Average	**0.100**	**0.117**	**0.146**	**0.185**

As an example, the time-histories of the tower's displacements under the EQ3 earthquake (the strongest among the earthquakes considered in Table 5) are displayed in Figure 11. It should be noted that EQ3 belongs to both the sets of spectrum-consistent earthquakes considered for the LP and the CP limit states. Fig. 12 shows the stress contours under the same earthquake. To evidence the zones where stress exceeded the tensile strength limit adopted in the non-linear model (that is 0.6 MPa, see Section 5) the colour scale in Fig. 12 was suitably set. This makes Fig. 12 showing a prediction of the damage pattern (purple zones) under tensile stress, which is along the S-W

edge of the tower. The non-linear analysis carried out under the same earthquake showed that this prediction is conservative since tensile damage affects only the bottom part of this edge (see Sect. 5).

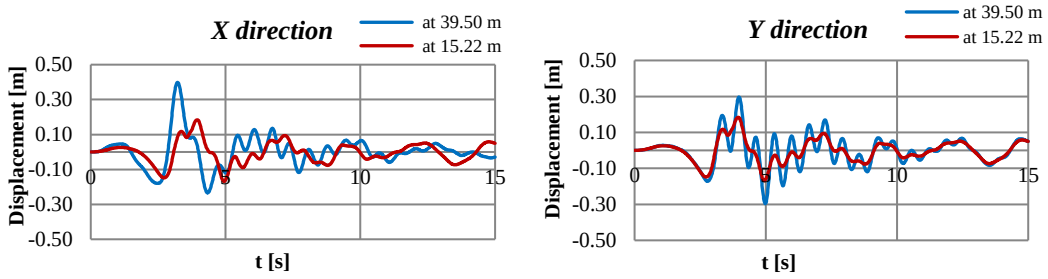

Figure 11. *Time-histories of displacements in the (a) x direction and (b) y-direction under EQ3.*

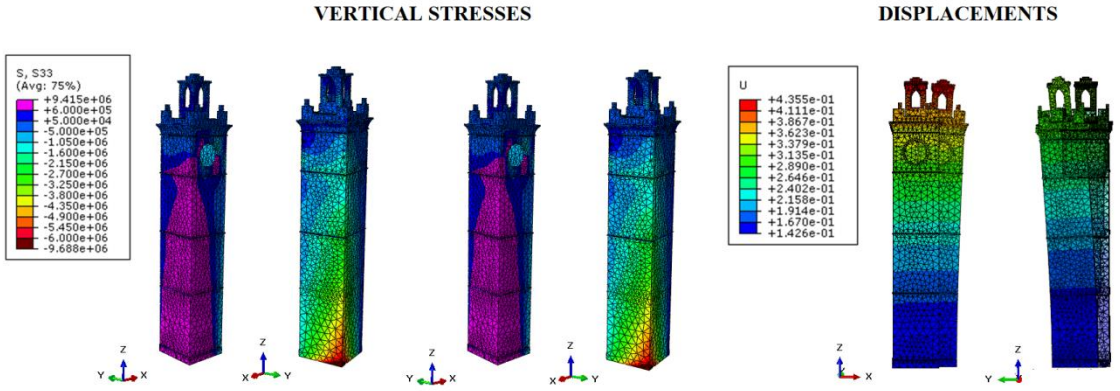

Figure 12. *Vertical stresses and horizontal displacements obtained from THLA under EQ3.*

4.3 Maximum displacements of the tower from the linear analyses

A comparison between the results presented in Table 6 and Table 8 shows that the RSMA generally underestimates the horizontal displacements of the tower obtained from THLA under the different earthquakes. The averaged values calculated from THLA are from 1.5 to 5 times greater than those obtained from RSMA. Underestimating displacements can have serious consequences for instance when the pounding phenomenon is concerned.

To assess the pounding phenomenon between the L'Aquila tower and the adjacent Margherita palace, the peak displacements of the palace in the two directions x and y should be considered, the tower and the palace bordering along two sides. Although the seismic behaviour of Palazzo Margherita was not investigated in this paper, the maximum horizontal displacement of the palace can be inferred from [7], where a displacement of about 0.028 m was calculated in both the x and the y directions at the LP limit state. Therefore, according to the results provided in Table 6 for the RMSA, a joint of at least (0.028+0.02) m = 0.048 m should be ensured to avoid the pounding effects at the LP limit state. On the other hand, when the averaged results of the LTHA are

accounted for (Table 8), the joint should be at least (0.028+0.10) m = 0.128 m, resulting in about three times the value obtained from the RSMA. It is to note that the tower and the palace do not reach their maximum displacements at the same time. Thus, a conservative estimate of the joint depth is made when summing up the maximum displacement values of these two structures. Of course, to prevent the pounding phenomenon it would be better considering the values calculated for the C limit state.

Less accurate as it is, RSMA is expected to be more conservative than THLA. On the contrary, it is found here to lead to underestimating the pounding effects compared to the more precise THLA.

5. Non-linear analyses

5.1 Non-linear behavior of masonry

A Concrete Damage Plasticity (CDP) model was assumed to describe the masonry non-linear behaviour, as allowed by ABAQUS. Initially thought for concrete structures under cyclic loads [42], the CDP model is in fact often adopted for masonry structures [21], [30], [36], [44], [43]. By assuming an isotropic behaviour of the material, CDP considers the degradation of elastic stiffness induced by plastic deformation both in tension and in compression. The mechanical parameters adopted to implement the CDP model in ABAQUS are listed in Table 9. The default values proposed by ABAQUS for eccentricity (0.1), shape factor Kc (2/3) and compressive yield ratio $Fb0/fc0$F (1.16) are assumed in the present model also in agreement to literature [21][29]. It can be briefly recalled that the compressive yield ratio is the ratio between the ultimate compressive strength in a biaxial state and the ultimate compressive strength in uniaxial condition, while the shape factor is a parameter that modifies the failure surface of the Drucker-Prager criterion, making it approximate the shape of the Mohr-Coulomb failure surface. The dilatation angle which controls the ductility was set to 10 as usually done for existing structures; the viscosity was kept very low to speed convergence according to [34][44].

The uniaxial post-elastic constitutive lows assumed in compression and in tension for the tower's masonry are depicted in Figures 16a and 16b respectively. A three-linear curve was adopted in tension, while the stress-strain curve in compression was assumed to be made by a first linear elastic branch followed by a hardening branch, a softening branch and a final constant-stress branch as usually done in the literature [34]. These stress-strain curves are obtained in agreement with the values given in Table 10. By interpolating experimental results obtained from a flat jack test performed in 2012 on behalf of the Municipality of L'Aquila, a compression yield strength of about 9 MPa was found [7]. Figure 15a shows the zone where the flat jack was inserted while Fig. 15b provides the experimental diagram obtained by the test. For the sake of

conservativeness, a value of 6 MPa is here assumed as compression elastic strength while a value of 8 MPa was set at the end of the hardening branch (see Figure 16a). Both these values fall within the range of conventional values (5.8÷8.2 MPa) provided by the Italian regulation [13] for masonry made by stone squared blocks. The tensile strength was assumed to be 1/10 of the compressive strength (that is 0.6 MPa), as typically done in the literature [30] [43][44]. Being the value of the initial elastic modulus $E = 3286.5\ MPa$ (see Table 4), the yield deformation under compression and under tension were $\varepsilon_{cy} = 6\ /3286.5\ =\ 0.0018$ and $\varepsilon_{ty} = 0.6\ /3286.5\ =\ 0.00018$ respectively.

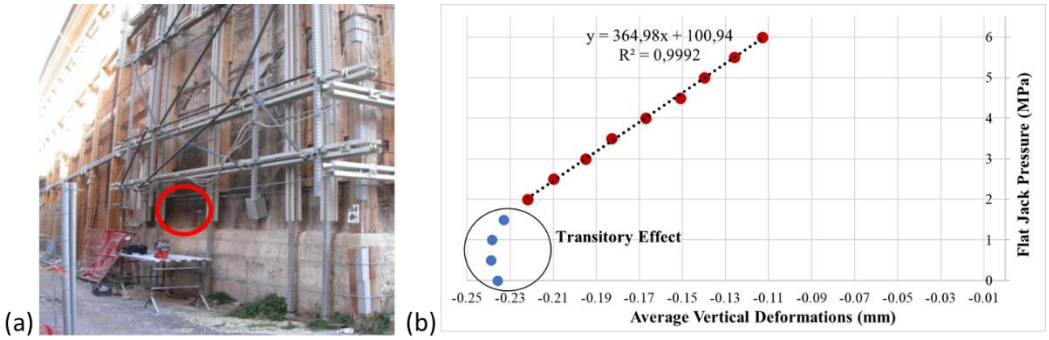

Figure 15. *(a) Zone where the flat jack test was performed; (b) stress-strain diagram obtained.*

Table 9. *Mechanical parameters of the CDP model adopted in ABAQUS*

Dilatation angle	Eccentricity	Fb0/fc0	Kc	Viscosity
10°	0.1	1.16	0.667	5E-005

Table 10. *Stress/strain values adopted for the uniaxial stress-strain curves*

	Compression					Tension			
strain	0	0.018	0.0054	0.0108	0.1	0	0.0001825	0.0002182	0.1
stress	0	6	8	1	1	0	0.6	0.0005	0.0005

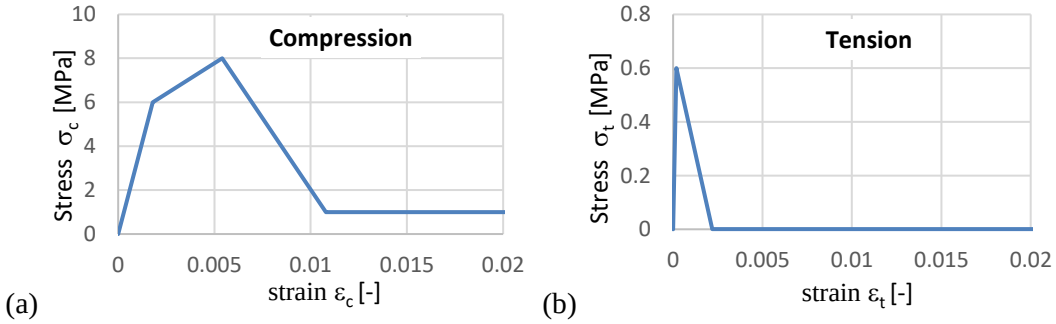

Figure 16. *Compression (a) and tension (b)uniaxial stress-strain behaviour of masonry adopted for the damage plasticity model (CDP model) in ABAQUS.*

It is worth noting that the value of tensile strength here assumed (0.6 MPa) is within the range of the values (0.04÷3.6 MPa) adopted in the literature for ancient masonry when exploiting the CDP model. In fact, a tensile strength of 0.04 MPa (about 1/60 of the assumed compressive strength) was set in [21] for clay bricks with very poor mechanical properties of the joints and quite regular courses; 0.12 MPa (1/20 of compressive strength) was taken in [30] when dealing with clay bricks and poor mortar; 0.2 MPa (1/10 of compressive strength) was assumed in [30] for clay masonry and lime mortar; 1.2 MPa (about 1/10 of the compressive strength) was assumed in [44] for masonry made of travertine stones; 1.5 MPa and 3.6 MPa (both being 1/10 of the relevant compressive strength) were considered in [43] for cut stone and coarse stone masonry of a historical minaret respectively. Of course, should a lower tensile strength be assumed for the L'Aquila tower (for instance 1/30 or even 1/60 of the compressive strength), this is expected to widen the damage pattern in the structure.

5.2 Time-history non-linear analyses (THNLAs)

A non-linear time-history analysis was carried out under the EQ3 earthquake. Two different analyses were carried out: the former neglecting the vertical component of the EQ3 earthquake and the latter accounting for it. It is to note that no significant difference was found between the horizontal displacements obtained from the two analyses. Figure 17 shows the time-history of the displacements in the x and y direction at 15.22 (palace roof level) and 39.50 (tower's top) respectively.

The maximum displacements obtained from the THNLA and the THLA under the EQ3 earthquake are compared in Table 11. The results show that linear and non-linear analyses lead to assess a very similar displacement demand on the tower, despite the time-histories are quite different (as can be inferred by comparing Figure 11 and Figure 17). This is not unexpected indeed, since an equal-displacement rule was found to be valid for flexible structures by well-known empirical studies 0. Although such a rule was proved to be met by single-degree-of-freedom systems, the present results show that it can be extended also to continuous slender cantilever structures. This means that a linear time-history analysis could be able to catch quite well the inelastic displacement demand of masonry towers under strong earthquakes.

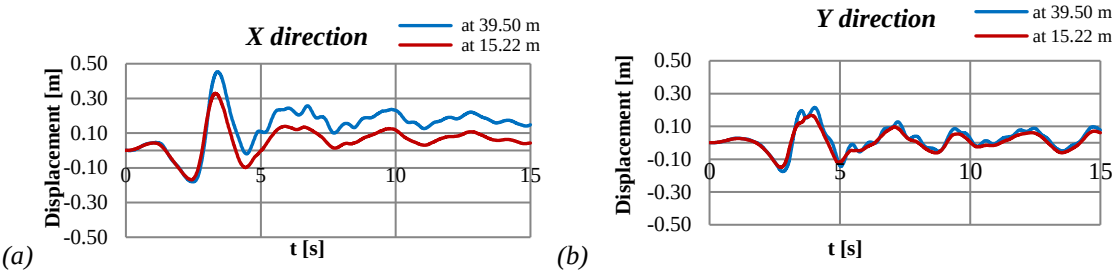

Figure 17. Non-linear analysis. Displacements of the tower in the (a) x direction and (b) y-direction under EQ3.

Table 11. *Maximum displacements obtained from the THNLA and THLA under EQ3.*

	Tower level			
	15.22 m		**39.50 m**	
	Ux (m)	Uy (m)	Ux(m)	Uy (m)
THNLA	**0.324**	**0.179**	**0.438**	**0.265**
THLA	0.306	0.184	0.398	0.297

Figures 18a and 18b show a map of damage under tension obtained at the end of the simulation, either when the vertical component of the earthquake is considered or not. Similarly, Fig. 19 shows the maps of the parameter ACYield, which indicates the elements that are plasticized under traction (value 1) and those that remain in the elastic range (values less than 1). It is worth noting that the vertical component of the earthquake produces very slight changes to the damage map, which confirms again that the contribution of the vertical ground motion can be neglected when this kind of structures are involved. The numerical simulation also showed that the tension damage affects a large part of the S-W edge of the tower, these findings being in good agreement with the crack pattern detected on the structure [8]. A comparison with Fig. 12 finally evidences that the linear analysis under EQ3 overestimated the spread of damage along the S-W edge of the tower.

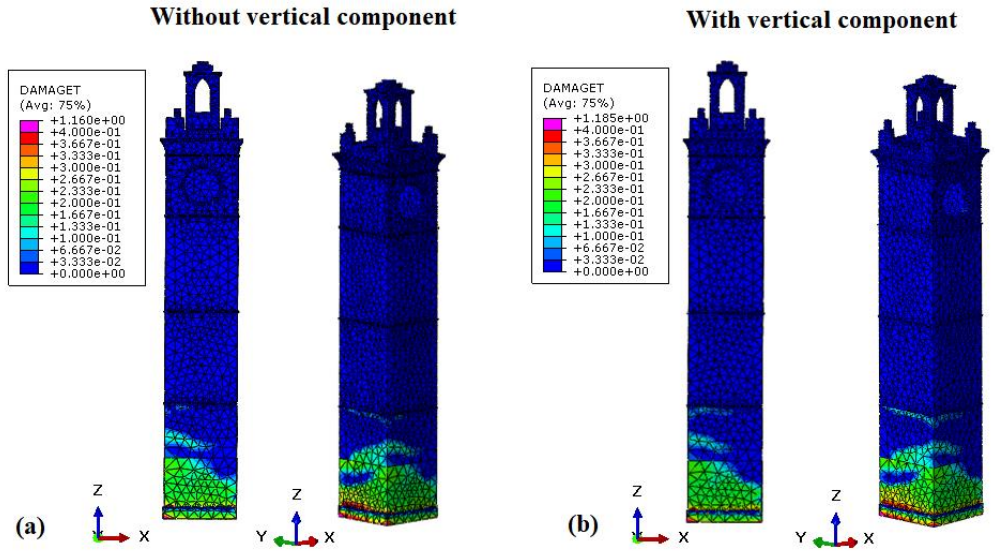

Figure 18. *Damage maps (DamageT) under EQ3 (a) without and (b) with the vertical component of the earthquake.*

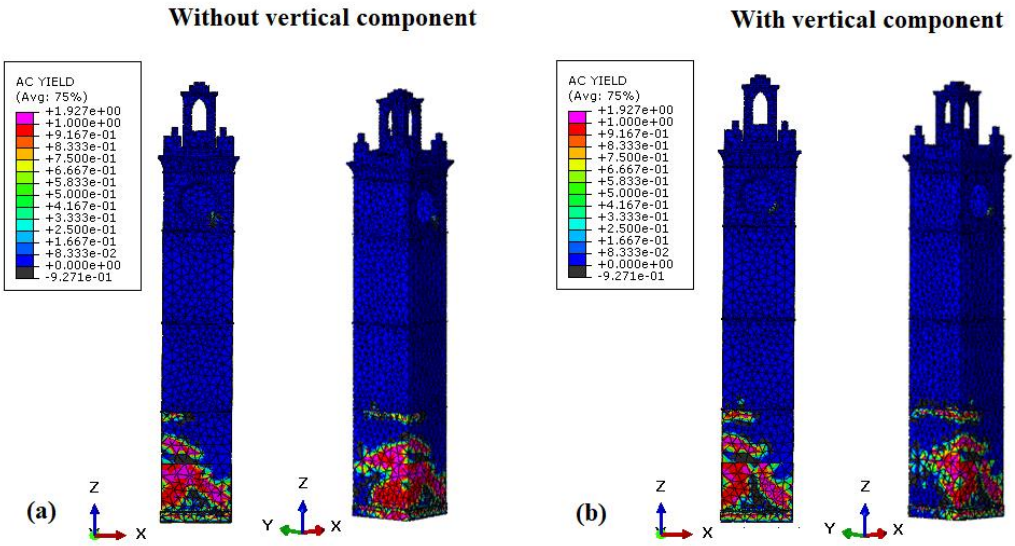

Figure 19. *Damage maps (ACYield) under EQ3 (a) without and (b) with the vertical component of the earthquake.*

6. Conclusions

Some key features of the identification process as well as the impact of the kind of dynamic analysis adopted when assessing the seismic behaviour of historical monuments were addressed in this paper. The medieval Civic Tower of L'Aquila was considered as a case-study in which the role of the identification process is paramount to overcome lack and discrepancy of data. An iterative identification procedure was performed over three different geometrical configurations of the tower and suitable ranges of elastic and inertial parameters. This led to find a representative geometrical and mechanical model of the monument. Some insights about criticisms and

strategies for the full identification of higher modes in such kinds of structures were discussed. Based on the identified model, the displacement demand was computed through the two code-compliant linear dynamic methods of analysis, namely the response spectrum modal analysis (RSMA) and the time-history linear analysis (THLA). All analyses were performed both for the life protection (LP) and the collapse prevention (CP) limit states. Two sets of seven spectrum-consistent earthquakes were considered for this purpose.

It was found that the RSMA may strongly underestimate the seismic displacement demand both for the LP and CP limit states. When assessing the dimension of the joint between the tower and the adjacent Palazzo Margherita to avoid the pounding phenomenon, the THLA gave, in fact, values even three times greater on average than those predicted by the RSMA. This is a criticism of the code-compliant RSMA that, being more approximate than the THLA, should be more conservative than –or at least as conservative as- the latter, to guarantee a safe design.

The impact of the vertical component of the earthquake was also evaluated. It was found that neither the displacement demand obtained from the MRSA nor that taken from the THLA were affected by the vertical component of the earthquake. As calculated from the THLA, the vertical stress increment due to the vertical component of the earthquake was found to be on average less than 5% for the LP limit state and less than 7% for the CP limit state. Although some recent studies evidenced a possible influence of the vertical ground motion on the seismic response of tall and slender structures, the present findings showed that the vertical component of the ground motion may reasonably be neglected when assessing the seismic behaviour of structures like the Civic tower of L'Aquila, as the design regulations in fact recommend doing.

A non-linear time-history analysis (THNLA) of the structure under the strongest earthquake among those considered showed that the vertical ground motion plays a very marginal role even on the post-elastic behaviour of the tower. The displacement demand was found very similar to that predicted by the linear time-history analysis under the same earthquake. This is in agreement with the well-known equal-displacement empirical rule valid for flexible single degree-of-freedom systems and means that a linear time-history analysis could be able to catch quite well the inelastic displacement demand of masonry towers under strong earthquakes. On the other hand, a good -although conservative with respect to the results of the THNLA- prediction of the damaged zones of the tower under tensile stresses was obtained through the THLA. A THNLA should be however preferably carried out to obtain a more realistic map of damage under a given earthquake. Performing non-linear dynamic analyses is in fact the best way to assess the seismic behaviour of structures allowing to predict the most vulnerable parts of them, which can be exploited to improve the effectiveness of the extraordinary maintenance of historical buildings.

Acknowledgements: The authors are very grateful to the Municipality of L'Aquila for the data kindly provided.

References

[1] De Stefano, A., Matta, E., & Clemente, P. (2016). Structural health monitoring of historical heritage in Italy: some relevant experiences. *Journal of Civil Structural Health Monitoring*, 6(1), 83-106.

[2] Lagomarsino, S., & Podesta, S. (2004). Seismic vulnerability of ancient churches: I. Damage assessment and emergency planning. *Earthquake Spectra*, 20(2), 377-394.

[3] Clementi, F., Gazzani, V., Poiani, M. and Lenci, S. (2016). Assessment of seismic behaviour of heritage masonry buildings using numerical modelling. *Journal of Building Engineering*, 8, pp.29-47.

[4] Porcu, M. C. (2017). Ductile behavior of timber structures under strong dynamic loads. *Wood in Civil Engineering*. Rijeka: InTechOpen, 173-196.

[5] Palermo, M., Silvestri, S., Gasparini, G., Baraccani, S. and Trombetti, T., 2015. An approach for the mechanical characterisation of the Asinelli Tower (Bologna) in presence of insufficient experimental data. *Journal of Cultural Heritage*, 16(4), pp.536-543.

[6] M. Dessalvi, M. C. Porcu, and M. Saba (2017), "Numerical analysis of the medieval Civic Tower of L 'Aquila to prevent seismic pounding effects, ANIDIS 2017 Procedia.

[7] Municipality of L'Aquila, "Relazioni tecniche ed elaborati grafici relativi alla ricostruzione del Palazzo Margherita e della Torre Civica redatti dall'assessorato alla ricostruzione dei beni culturali del comune di L'Aquila," 2012, in Italian.

[8] Cimellaro, G. P., Salluzzo, G., Piantà, S., & De Stefano, A. (2010). Nonlinear modeling of L'Aquila civic tower. In 14th European Conference on Earthquake Engineering (14ECEE).

[9] Cimellaro, G. P., Piantà, S., & De Stefano, A. (2012). Output-only modal identification of ancient L'Aquila city hall and civic tower. *Journal of Structural Engineering*, 138(4), 481-491.

[10] Lorenzoni, F., Aoki, T., Casarin, F., Modena, C., Da Porto, F., Sabia, D., & Sumini, V. M. A. (2012). Post-Earthquake assessment of the civic tower in L'Aquila: ambient vibration tests and structural health monitoring. In SAHC 2012 (8th international conference on structural analysis of historical constructions), pp. 1612-1620, DWE.

[11] Cimellaro, G. P., Christovasilis, I. P., Reinhorn, A. M., De Stefano, A., & Kirova, T. (2010). L'Aquila earthquake of April 6th, 2009 in Italy: rebuilding a resilient city to multiple hazard. MCEER Technical Rep.—MCEER-10.

[12] Salem, H., Gregori, A., Helmy, H., Fassieh, K., & Tagel-Din, H. (2017). Seismic assessment of damaged Margherita palace using applied element method. In 16th World Conference on Earthquake Engineering, 16WCEE.

[13] D.M 17 gennaio 2018, Aggiornamento delle Norme tecniche per le Costruzioni, Suppl. Ordin. alla "Gazzetta Uff. n. 42 del 20 febbraio 2018- Ser. Gen., 2018.

[14] CEN, "EN8-1 General rules, seismic actions and rules for buildings Eurocode," vol. 3, no. 121124, 2003.

[15] Porcu, M. C., Bosu, C., & Gavrić, I. (2018). Non-linear dynamic analysis to assess the seismic performance of cross-laminated timber structures. *Journal of Building Engineering*, vol.19, 480-493.

[16] Vielma-Perez J.C., Porcu M.C., Gomez-Fuentes M.A. (2020), Non-linear analyses to assess the seismic performance of RC buildings retrofitted with FRP, *Revista Internacional de Métodos Numéricos para Cálculo y Diseño en Ingeniería*, vol. 36, (2), 24.

[17] Porcu, M. C., Vielma, J. C., Panu, F., Aguilar, C., & Curreli, G. (2019). Seismic retrofit of existing buildings led by non-linear dynamic analyses. *International Journal of Safety and Security Engineering*, 9(3), 201-212.

[18] Valente, M., & Milani, G. (2016). Non-linear dynamic and static analyses on eight historical masonry towers in the North-East of Italy. *Engineering Structures*, 114, 241-270.

[19] Penna, A., Rota, M., Mouyiannou, A., & Magenes, G. (2013). Issues on the use of time-history analysis for the design and assessment of masonry structures. Proc. COMPDYN2013.

[20] Vielma, J.C., Porcu, M.C., López, N. (2020) Intensity Measure Based on a Smooth Inelastic Peak Period for a More Effective Incremental Dynamic Analysis. *Applied Sciences*, *10*, 8632.

[21] Valente, M. and Milani, G., 2016. Seismic assessment of historical masonry towers by means of simplified approaches and standard FEM. Construction and Building Materials, 108, pp.74-104.

[22] Bartoli, G., Betti, M. and Monchetti, S., 2017. Seismic risk assessment of historic masonry towers: comparison of four case studies. *Journal of Performance of Constructed Facilities*, 31(5), p.04017039.

[23] Invernizzi, S., Lacidogna, G., Lozano-Ramírez, N.E. and Carpinteri, A., 2019. Structural monitoring and assessment of an ancient masonry tower. *Engineering Fracture Mechanics*, 210, pp.429-443

[24] Casolo, S., Milani, G., Uva, G. and Alessandri, C., 2013. Comparative seismic vulnerability analysis on ten masonry towers in the coastal Po Valley in Italy. *Engineering Structures*, 49, pp.465-490.

[25] Ferrante, A., Loverdos, D., Clementi, F., Milani, G., Formisano, A., Lenci, S. and Sarhosis, V., 2021. Discontinuous approaches for nonlinear dynamic analyses of an ancient masonry tower. *Engineering Structures*, 230, p.111626.

[26] Casolo S., A three-dimensional model for vulnerability analysis of slender medieval masonry towers *J. Earthq. Eng.*, vol. 2, no. 4, pp. 487–512, 1998, doi: 10.1080/13632469809350332.

[27] D'Ambrisi, A., Mariani, V. and Mezzi, M., 2012. Seismic assessment of a historical masonry tower with nonlinear static and dynamic analyses tuned on ambient vibration tests. *Engineering Structures*, 36, pp.210-219.

[28] Milani, G. and Clementi, F., 2021. Advanced seismic assessment of four masonry bell towers in Italy after operational modal analysis (OMA) identification. *International Journal of Architectural Heritage*, 15(1), pp.157-186.

[29] Jain, A., M. Acito, C. Chesi, and E. Magrinelli (2020). The seismic sequence of 2016–2017 in Central Italy: a numerical insight on the survival of the Civic Tower in Amatrice, *Bulletin of Earthquake Engineering* , 18, no. 4, 1371-1400.

[30] Acito M., Chesi C., Milani G., and S. Torri, Collapse analysis of the Clock and Fortified towers of Finale Emilia, Italy, after the 2012 Emilia Romagna seismic sequence: Lesson learned and reconstruction hypotheses, *Construction and Building Materials*, vol. 115, pp. 193–213, 2016, doi: 10.1016/j.conbuildmat.2016.03.220.

[31] Castellazzi, G., D'Altri, A.M., de Miranda, S., Chiozzi, A. and Tralli, A., 2018. Numerical insights on the seismic behavior of a non-isolated historical masonry tower. *Bulletin of Earthquake Engineering*, 16(2), pp.933-961.

[32] Smoljanović, H., Nikolić, Z., Zivaljic, N. (2013). Overview of the methods for the modelling of historical masonry structures. *Gradevinar 65, 603-618.*

[33] Angelillo, M., Lourenço, P. B., & Milani, G. (2014). Masonry behaviour and modelling. In *Mechanics of masonry structures* (pp. 1-26). Springer, Vienna.

[34] Bayraktar, E. Hökelekli, F. M. Halifeoğlu, A. Mosallam, and H. Karadeniz, "Vertical strong ground motion effects on seismic damage propagations of historical masonry rectangular minarets," *Eng. Failure Analysis*, vol. 91, no. April, pp. 115–128, 2018, doi: 10.1016/j.engfailanal.2018.04.029.

[35] Abaqus/CAE, Simulia. http://www.3ds.com/products/simulia/portfolio/abaqus.

[36] Diaferio, M., Foti, D. and Potenza, F., 2018. Prediction of the fundamental frequencies and modal shapes of historic masonry towers by empirical equations based on experimental data. *Engineering Structures*, 156, pp.433-442.

[37] Pieraccini, M., Dei, D., Betti, M., Bartoli, G., Tucci, G. and Guardini, N., 2014. Dynamic identification of historic masonry towers through an expeditious and no-contact approach: Application to the "Torre del Mangia" in Siena (Italy). Journal of Cultural Heritage, 15(3), pp.275-282.

[38] Paglietti, A. & Porcu, M. C. (2001). Rigid–plastic approximation to predict plastic motion under strong earthquakes. Earthquake engineering & structural dynamics, 30(1), 115-126.

[39] Iervolino, I., Galasso, C. and Cosenza, E, REXEL: computer aided record selection for code-based seismic structural analysis. *Bulletin of Earthquake Engineering*, 8(2), pp.339-362, 2010.

[40] Ambraseys N., Smit, P., Douglas, J., Margaris, B., Sigbjörnsson et al., Internet site for European strong-motion data. *Bollettino di Geofisica Teorica ed Applicata*, 45(3), 113-129, 2004.

[41] Porcu M.C. (2017). Code inadequacies discouraging the earthquake-based seismic analysis of buildings, *Int. J. of Safety and Security Engineering*, vol. 7, n. 4, pp. 545–556, doi:10.2495/SAFE-V7-N4-545-556.

[42] Lee, Jeeho, and Gregory L. Fenves (1998), Plastic-damage model for cyclic loading of concrete structures. *Journal of Engineering Mechanics,* 124, no. 8: 892-900

[43] E. Ercan, B. Arisoy, E. H. İ, and A. N. Ğ. Lu, Estimation of Seismic Damage Propagation in a Historical Masonry Minaret, Sigma *J. Eng. Nat. Sci.*, vol. 35, no. 4, pp. 647–666, 2017.

[44] Bertolesi E, Milani G, Lopane FD and Acito M (2017) Augustus Bridge in Narni (Italy): seismic vulnerability assessment of the still standing part, possible causes of collapse, and importance of the Roman concrete infill in the seismic-resistant behavior. *Int J Architectural Heritage*, 11–5:717–746.

[45] Miranda E. & Bertero V.: Evaluation of Strength Reduction Factors for Earthquake-Resistant Design. *Earthquake Spectra*. Vol 10, No. 2, 1994.